

Enhanced accretion rates of stars on Super-massive Black Holes by star-disk interactions in galactic nuclei

Andreas Just¹, Denis Yurin^{2,1}, Maxim Makukov^{2,1}, Peter Berczik^{3,1,5}, Chingis Omarov^{2,1},
Rainer Spurzem^{3,1,4}, and Emanuel Y. Vilkoviskij²

¹*Universität Heidelberg, Zentrum für Astronomie, Astronomisches Rechen-Institut, Mönchhof-Straße 12-14,
69120 Heidelberg, Germany*

just@ari.uni-heidelberg.de

²*Fesenkov Astrophysical Institute, Observatory 23, 050020 Almaty, Kazakhstan*

³*National Astronomical Observatories of China, Chinese Academy of Sciences, 20A Datun Rd., Chaoyang
District, Beijing 100012, China*

⁴*Kavli Institute for Astronomy and Astrophysics, Peking University, China*

⁵*Main Astronomical Observatory, National Academy of Sciences of Ukraine, MAO/NASU, 27 Akademika
Zabolotnoho St. 03680 Kyiv, Ukraine*

ABSTRACT

We investigate the dynamical interaction of a central star cluster surrounding a super-massive black hole and a central accretion disk. The dissipative force acting on stars in the disk leads to an enhanced mass flow towards the super-massive black hole and to an asymmetry in the phase space distribution due to the rotating accretion disk. The accretion disk is considered as a stationary Keplerian rotating disk, which is vertically extended in order to employ a fully self-consistent treatment of stellar dynamics including the dissipative force originating from star-gas ram pressure effects. The stellar system is treated with a direct high-accuracy N -body integration code. A star-by-star representation, desirable in N -body simulations, cannot be extended to real particle numbers yet. Hence, we carefully discuss the scaling behavior of our model with regard to particle number and tidal accretion radius. The main idea is to find a family of models for which the ratio of two-body relaxation time and dissipation time (for kinetic energy of stellar orbits) is constant, which then allows us to extrapolate our results to real parameters of galactic nuclei. Our model is derived from basic physical principles and as such it provides insight into the role of physical processes in galactic nuclei, but it should be regarded as a first step towards more realistic and more comprehensive simulations. Nevertheless, the following conclusions appear to be robust: the star accretion rate onto the accretion disk and subsequently onto the super-massive black hole is enhanced by a significant factor compared to purely stellar dynamical systems neglecting the disk. This process leads to enhanced fueling of central disks in active galactic nuclei and to an enhanced rate of tidal stellar disruptions. Such disruptions may produce electromagnetic counterparts in form of observable X-ray flares. Our models improve predictions for their rates in quiescent galactic nuclei. We do not yet model direct stellar collisions in the gravitational potential well of the black hole, which could further enhance the growth rate of the black hole. Our models are relevant for quiescent galactic nuclei, because all our mass accretion rates would give rise to luminosities much smaller than the Eddington luminosity. To reach Eddington luminosities, outflows and feedback as in the most active QSO's other scenarios are needed, such as gas accretion after galaxy mergers. However, for AGNs close to the Eddington limit this process may not serve as the dominant accretion process due to the long timescale.

Subject headings: accretion disks - galaxies, galactic nuclei - celestial mechanics - stellar dynamics, N -body simulations

1. Introduction

Kinematic and photometric data of galactic nuclei have revealed that super-massive central black holes (SMBHs) are ubiquitous in most galaxies (see e.g. Kormendy & Richstone 1995 for a review). Detailed information on their photometric profiles and shapes of spectral line profiles allow us, in certain limits, to deduce the true shape of the distribution function in phase space of such systems. The distribution function determines the rate at which stars will come close to the SMBH, be tidally disrupted or destroyed by direct collisions and eventually accreted onto the black hole (Frank & Rees 1976; Bahcall & Wolf 1976). Quasars, however, which are the most luminous witnesses of accretion activity onto SMBHs are observed already in the young universe at redshifts of $z > 5$. It is difficult to explain how black holes can grow so quickly to the observed high masses ($10^6 - 10^9 M_\odot$) by pure star accretion. It has been therefore argued that massive seed black holes form already by dissipative and viscous collapse, possibly accompanied by the formation of massive stars and their coalescence, at the time of galaxy formation (Colgate 1967; Spitzer & Saslaw 1966; Spitzer & Stone 1967; Sanders 1970; Rees 1984). In the hierarchical picture of galaxy formation, the most massive dark halos with small angular momentum can account for the early formation of the most massive black holes. The SMBH forms by a centrally focused collapse entering a phase of a dense super-massive gaseous object which is supported by star-gas interactions (Bisnovatyi-Kogan & Syunyaev 1972; Vilkoviskij 1975; Hara 1978; Langbein et al. 1990). The interaction of a compact stellar cluster with a massive central object in the form of a superstar or SMBH was considered by Vilkoviskij (1975); Hills (1975); Hara (1978). The evolution of the dense non-rotating stellar cluster was studied by Spitzer & Saslaw (1966); Bisnovatyi-Kogan (1978) among others, and the evolution of the gas sphere was considered by Langbein et al. (1990).

These studies have commonly neglected angular momentum, which should not be neglected during mergers nor in the intrinsic structure of galaxies. Spectra of active galactic nuclei suggest that there should be gas in the form of a massive central accretion disk (AD) in which all interstellar matter

settles before it may be accreted. The origin of the AD could be inflowing cool gas during mergers and/or debris by direct stellar collisions or stellar evolutionary processes, depending on the evolutionary state of the host galaxy. Artymowicz et al. (1993) provide a theoretical model framework in which star-gas interactions and the build-up of massive stars generate a massive AD around the central SMBH.

Recent work shows that gaseous disks in galactic centers around SMBHs are important for the dynamics and the morphology of central regions of galaxies and for the evolution of single or multiple central black holes in many ways. For example Cuadra et al. (2009); Callegari et al. (2009, 2011) study the role of small scale disks for the acceleration of binary black hole mergers, through dissipation of kinetic energy in the disk, after a galactic merger. Baruteau et al. (2011) discuss the hardening of stellar binaries in circumnuclear disks and their subsequent interactions with central black holes, which may lead to high velocity stellar escapers.

Shakura & Sunyaev (1973) developed a model for a stationary AD, which has been the basis of many investigations since then. Close to the inner boundary of the AD, at a few Schwarzschild radii r_s , general relativistic effects must be taken into account. Novikov & Thorne (1973) extended the standard disc model in that regime.

If the inner part of the AD reaches a critical surface density the interaction of orbits with the gas (or more correctly energy and momentum transfer of stars due to ram pressure effects, henceforth denoted as dissipation) cannot be neglected anymore. Stellar interactions with accretion disks were also considered by Vilkoviskij & Bekbosarov (1982); Vilkoviskij (1983); Syer et al. (1991). More detailed investigations of the stellar orbits, crossing accretion disks were presented in Vokrouhlicky & Karas (1998) and in Šubr & Karas (1999). Šubr & Karas (1999) and Šubr et al. (2004) assumed an infinitely thin disk interacting with stars; they found that the interaction between the disk and the stars (star-gas dissipation) will deplete counter-rotating stars, create a flattening of the large-scale structure of the system and initiate anisotropies (i.e. changes of the eccentricity distributions). These studies did not take into account any feed-

back onto the disk or any finite-thickness effects of the disk. They tried to find a stationary state in which the transport of stars into the central galactic region is balanced by removal of stars from the central disk. Evolution timescales and initial conditions to reach this equilibrium was missing.

Around SMBHs the AD may extend to the parsec scale, orders of magnitude larger than r_S . Rauch (1995, 1999) studied in detail the impact of the AD on the orbits and the distribution of stars with test particle simulations. Their work includes relativistic effects, even for the case of rotating Kerr black holes. They find that the orbital inclination with respect to the AD declines quickly as soon as the dissipative force becomes effective. Additionally they find a steepening of the central density cusp, due to the combined effect of relativistic orbit migration and stellar collisions.

The semi-analytic model by Vilkoviskij & Czerny (2002) raises the point that two-body relaxation of the stars within and near the disk will tend to elevate trapped stars again out of the disk, and that the competition between relaxation and dissipation will define a stationary state of the system, with some well-defined stationary flux of stars going down to the black hole. Vilkoviskij & Czerny (2002) compared the star-star two-body interactions with the star-disk interactions and concluded that the latter is stronger in the inner parts of the accretion disk and vice versa in the outer parts based on nearly circular orbits of the stars. They derived analytic approximations for the effective inclination of stellar orbits, where the inflow to the SMBH takes place. They also derived a critical radius inside which direct stellar collisions must be taken into account.

All of the mentioned papers so far have both strong and weak points. Rauch (1999) is the only paper to combine general relativity effects and stellar collisions, but considered only the central region where the (spherically symmetric) potential is dominated by the super-massive black hole. They used an approximate model of stellar dynamics based on a Monte Carlo technique, which requires a spherically symmetric central star cluster. In Rauch (1995) they combined relativistic effects with star-disk interactions, but the disk is assumed to be infinitely thin. The infinitely thin disk approximation was also used in other

work by Šubr & Karas (1999); Šubr et al. (2004); Vilkoviskij & Czerny (2002)).

Following the ideas of Vilkoviskij & Czerny (2002) we investigate by self-consistent direct N -body simulations, the interaction of a central compact stellar cluster (CSC) with the AD in active galactic nuclei. We focus on the mutual interplay of two-body relaxation and the depletion of stars by the dissipative force in the AD as a secular long-term evolution of the stellar mass distribution and the velocity distribution function of the CSC. In this paper we report results on a new model of star-disk interactions in galactic nuclei. Our focus lies on the correct and accurate representation of the stellar orbital motion crossing the disk, by implementing a disk with its density distribution in a full three-dimensional N -body simulation. We have added the force and force time derivative to the standard Hermite scheme (see below) as a function of local disk density and velocity in three dimensions. This is the most general approach, and later it will allow us to include evolving models of the AD and appropriately model the mass and energy transfer between the AD and CSC.

Our first results concern the enhanced accretion rate onto the central SMBH due to the interaction with the AD, in the regime where the relaxation timescale is comparable to the dissipation timescale. This is, to our knowledge, the first approach to study the competition between relaxation and star-gas dissipation in a direct simulation. Since the direct simulations are not yet able to reach realistic particle numbers and spatial resolution, we will perform a careful scaling analysis to show in which way our numerical simulations have to be interpreted for real astrophysical galactic nuclei.

This paper is organized as follows: in Sect. 2 we describe the accretion disc and the dissipative force in detail, Sect. 3 gives the numerical realizations of the system, in Sect. 4 the results are discussed and in Sect. 5 a summary and conclusions are presented.

In follow-up papers we will discuss the dependence of the dissipation on the orbital parameters and the phase space evolution of the cusp stars in detail and take into account the feedback of the star-gas interaction on the AD properties. Detailed studies of migration of stars, binaries, and black holes inside the disk towards the cen-

ter, and its observational consequences will also be included in future work.

2. Physics of the accretion disk and the star-gas interactions

We consider an AGN model consisting of three subsystems: i) a compact stellar cluster (CSC) with mass M_{cl} describing the inner part of the galactic center. It is spherically symmetric, non-rotating, and in dynamical equilibrium. ii) An accretion disk (AD) with mass $M_{\text{d}} = \mu_{\text{d}} M_{\text{cl}}$. It is vertically extended, non-evolving, and has a Keplerian rotation curve. iii) A central super massive black hole (SMBH) with mass $M_{\text{bh}} = \mu_{\text{bh}} M_{\text{cl}}$. The motion of each star m_i of the CSC is determined by the mutual gravitational interaction of the stars, the gravitational force of the SMBH, and by a dissipative force \vec{F}_{d} from the AD. The equation of motion is given by

$$\ddot{\vec{r}}_i = - \sum_{i \neq j} \frac{Gm_j \vec{r}_{ij}}{r_{ij}^3} - \frac{GM_{\text{bh}} \vec{r}_i}{r_i^3} + \frac{\vec{F}_{\text{d}}}{m_i} \quad , \quad (1)$$

where $\vec{r}_{ij} = \vec{r}_i - \vec{r}_j$ with \vec{r}_i, \vec{r}_j the positions of stars i and j , respectively. Since the AD has a small mass compared to the black hole and the enclosed stellar cluster, we neglect the gravitating effect of the disk on the system. Numerical details for computing the forces are given in Sect. 3.

2.1. The accretion disk

We are interested in the dynamical action of the AD on the stellar component. Therefore we adopt a 3-dimensional axisymmetric stationary disk model, which is differentially rotating with the local circular velocity. For the inner structure and evolution of such disks see the review of Park & Ostriker (2001), and for the basic physics of accretion disks see e.g. Frank et al. (2002). A widely used model for the AD is the model of Shakura & Sunyaev (1973), with the radial scaling described in detail in Novikov & Thorne (1973, hereafter NT), which was also used by Rauch (1995); Vilkoviskij & Czerny (2002).

For the radial profile of the AD the surface density Σ is given by

$$\Sigma(R) = \Sigma_{\text{d}} \left(\frac{R}{R_{\text{d}}} \right)^{-\alpha} \quad \text{with} \quad \alpha = 3/4, \quad (2)$$

where $R^2 = x^2 + y^2$, R_{d} is the cut-off radius of the disk and Σ_{d} is the surface density at the cut-off radius. The value $\alpha = 3/4$ corresponds to the outer disk range of NT. The mass M_{d} of the disk is

$$M_{\text{d}} = 2\pi \int_0^{R_{\text{d}}} \Sigma(R) R dR = \frac{2\pi}{2-\alpha} \Sigma_{\text{d}} R_{\text{d}}^2. \quad (3)$$

For the numerical integration using the 4th order Hermite scheme we need a smooth force in space. Therefore we introduce a continuous but steep outer cutoff by

$$\Sigma(R) = \Sigma_{\text{d}} \left(\frac{R}{R_{\text{d}}} \right)^{-\alpha} \exp \left[-\beta_{\text{s}} \left(\frac{R}{R_{\text{d}}} \right)^s \right], \quad (4)$$

In order to retain exactly Eq. 3 for the total disk mass (with the integral now up to ∞) we choose

$$\beta_{\text{s}} = \left[\Gamma \left(1 + \frac{2-\alpha}{s} \right) \right]^{s/(2-\alpha)} \quad (5)$$

with the Gamma-function $\Gamma(x)$. For $s \rightarrow \infty$ the cutoff is discontinuous at $R_{\text{cut}} = R_{\text{d}}$ with $\beta_{\text{s}}^{(1/s)} \rightarrow 1$. We will use $s = 4$ leading to $\beta_{\text{s}} = 0.70$ for $\alpha = 3/4$. In this case the surface density at R_{d} is $\Sigma(R_{\text{d}}) = 0.49 \Sigma_{\text{d}}$.

An inspection of the scaling relations in NT shows that in the case of SMBHs self-gravity of the AD for the vertical structure becomes important for radii larger than $\sim 100 r_{\text{S}}$. Since we cannot resolve the innermost part of the AD we simplify the model of the vertical disk structure. We adopt a self-gravitating isothermal profile given by

$$\rho_{\text{g}}(R, z) = \frac{\Sigma(R)}{\sqrt{2\pi} h_z} \exp \left(-\frac{z^2}{2h_z^2} \right). \quad (6)$$

In the NT model the (half-)thickness h_z increases with distance according $\propto R^{9/8}$. Since this is altered by self-gravitation and since we cannot resolve the vertical structure of such a thin disc close to the inner boundary, we decided to adopt a constant thickness h_z , taking an appropriate value at some intermediate radius of the AD. To simplify the equations we define the dimensionless value $h = h_z/R_{\text{d}}$, which is also constant.

The effective sound speed c_{s} (which may be dominated by the turbulent motion in a clumpy gas) is given by (assuming a vertically isothermal

model)

$$\begin{aligned} c_s^2(R) &= 8\pi G\rho_g(R,0)h_z^2 = 4\sqrt{2\pi}G\Sigma h_z \quad (7) \\ &= \sqrt{\frac{8}{\pi}}(2-\alpha)\frac{\mu_d}{\mu_{bh}}h\left(\frac{R}{R_d}\right)^{1-\alpha}v_{\text{circ}}^2(R), \end{aligned}$$

where $v_{\text{circ}}(R)$ is approximated by the Kepler rotation of the SMBH only. In a thin disk the radial pressure support can be neglected. Eq. 7 shows that the rotation curve v_{circ} is highly supersonic ($v_{\text{circ}}/c_s \approx 100$ at the outer boundary R_d for the parameters used in our simulations: $\mu_{bh} = 0.1$, $\mu_d = 0.01$, $h = 10^{-3}$). The Mach number is increasing inwards.

The sound speed decreases with increasing radius and the stability of the AD is a function of radius. The Toomre Q stability parameter is given by

$$Q^2 = \left(\frac{\kappa c_s}{\pi G\Sigma}\right)^2 = \frac{8}{2-\alpha}\sqrt{\frac{2}{\pi}}\frac{\mu_{bh}}{\mu_d}h\left(\frac{R}{R_d}\right)^{\alpha-3} \quad (8)$$

with epicyclic frequency κ , which shows that heavy and thin ADs are unstable near the outer boundary. For the case of $\mu_d/\mu_{bh} = 0.1$ and $h = 10^{-3}$ the AD is formally unstable at $R > 0.26R_d$. In the framework of our simplified AD model with constant thickness we may ignore this instability, since it could easily be avoided by adopting an increasing thickness with distance R . With eqs. 2 and 3 the density distribution of the AD with constant thickness (Eq. 6) is given by

$$\begin{aligned} \rho_g(R, z) &= \frac{2-\alpha}{2\pi\sqrt{2\pi}}\frac{M_d}{hR_d^3}\left(\frac{R}{R_d}\right)^{-\alpha} \times \quad (9) \\ &\exp\left[-\beta_s\left(\frac{R}{R_d}\right)^s\right]\exp\left(-\frac{z^2}{2h^2R_d^2}\right). \end{aligned}$$

2.2. Dissipation of stellar kinetic energy

A detailed theory of the dissipative force working on the stars crossing the AD depends on the details of differential rotation, density profile, turbulent motion in the disk and possible resonance effects. Stars interact with the AD typically many times supersonically before they are finally trapped in it. Hence, we restrict our investigation to supersonic motion only, neglecting the details of the last few passages before trapping.

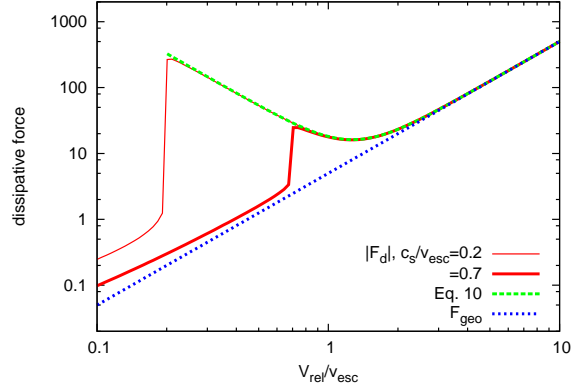


Fig. 1.— Drag force $|F_d|$ in units of $[\pi r_\star^2 \rho_g c_s^2]$ for different sound speeds c_s in the AD (full red lines). We have chosen $Q_d = 5$ and $\ln \Lambda = 13$. The dashed green line shows the approximation given in Eq. 10 for the first case. F_{geo} (dotted blue line) is used in the simulations.

In this case we can use for the dissipative force the geometrical cross section $F_{\text{geo}} = Q_d \pi r_\star^2 \rho_g V_{\text{rel}}^2$ (determined by the effective area $Q_d \pi r_\star^2$ of the bow shock with stellar radius r_\star and $Q_d \sim 5$) enhanced by dynamical friction, which is the gravitational pull by the over-density in the Mach cone due to gravitational focusing (Ostriker 1999). The dissipative force \vec{F}_d can be written in the form (Spurzem et al. 2004)

$$\begin{aligned} \vec{F}_d &= -\pi r_\star^2 \rho_g |\vec{V}_{\text{rel}}| \vec{V}_{\text{rel}} \left[Q_d + \left(\frac{v_{\text{esc}}}{V_{\text{rel}}}\right)^4 \ln \Lambda \right] \\ &\text{for } V_{\text{rel}} > c_s. \quad (10) \end{aligned}$$

Here v_{esc} is the escape velocity at the surface of the star ($v_{\text{esc}} = 620$ km/s for the Sun) and the relative velocity $\vec{V}_{\text{rel}} = \vec{V}_\star - \vec{V}_d$ is the velocity of the star in the frame co-rotating with the disc. Λ corresponds to the length of the Mach cone in units of the star radius r_\star leading to a Coulomb logarithm $\ln \Lambda \sim 10 - 20$.

Fig. 1 shows the dissipative force $|F_d|$ for a range of values of c_s/v_{esc} (full red lines). The dashed green line shows the approximation given in Eq. 10 for $c_s/v_{\text{esc}} = 0.2$. The contribution to the dissipative force by F_{geo} is shown by the dotted blue line. From the strong dominance of the dynamical friction for velocities V_{rel} smaller than

v_{esc} we expect that stars are quickly decelerated to $V_{\text{rel}} < c_s$ and onto co-rotating circular orbits which then move slowly to the center with a radial decay speed comparable to c_s . The dissipative force is anti-parallel to the relative velocity and can also be accelerating with respect to the rest frame of the CSC.

For a measure of the efficiency of the dissipative force we first introduce a dissipative time scale $t_{\text{diss}\star}$, which describes the energy change $\dot{E}_\star^{(\text{sd})}$ of a single star due to the dissipative force F_d arising from interaction with the AD at the outer part of the disk. Our ansatz is:

$$t_{\text{diss}\star} = \frac{\xi_k m_\star \sigma_\star^2}{P_d \dot{E}_\star^{(\text{sd})}} \quad (11)$$

with the stellar mass m_\star and the 3D stellar velocity dispersion σ_\star ; the dissipative time scale as defined above depends strongly on radius. At the outer edge R_d of the AD we have for example $\dot{E}_\star^{(\text{sd})} = Q_d \pi r_\star^2 \rho_g \sigma_\star^3$, $\rho_g = \Sigma_d / R_d$, $t_{\text{dyn}} = R_d / \sigma_\star$, and one gets

$$t_{\text{diss}\star}(R_d) = \frac{\xi_k}{Q_d P_d} \cdot \frac{\Sigma_\star}{\Sigma_d} \cdot t_{\text{dyn}} \quad (12)$$

In the second form of the above equation we have defined the surface density of stars $\Sigma_\star = m_\star / (\pi r_\star^2)$, which provides useful insights. Note that this dissipative time scale related to a single star is a strongly increasing function with radius, so the longest dissipation time can be found at the outer edge of the disk, in our case at R_d .

We consider now the quantities ξ_k and P_d . The former implicitly is defined by $2E_\star := \xi_k m_\star \sigma_\star^2(R_d) = G m_\star M_{\text{cl}} / R_d$. The latter, P_d , accounts for the number of disk passages that a star will need before its full kinetic energy is dissipated, and it also includes an average over the orbital parameters of the stars, which gives:

$$P_d = \left\langle g(e, i, R_d/p) \frac{t_{\text{dyn}}}{t_{\text{orb}}} \right\rangle \quad (13)$$

The average in the equation above is taken over the disk crossing events of all stars with the proper efficiency function $g(e, i, R/p)$ which depends on the orbital eccentricity e , the inclination with respect to the AD i , and the focal parameter p (the properties of $g(e, i, R/p)$ will be discussed in detail in a follow-up paper). For simplicity we neglect here the contribution by dynamical friction.

It can easily be included by replacing Q_d with the velocity dependent factor $(Q_d + (v_{\text{esc}}/V_{\text{rel}})^4 \ln \Lambda)$ in the definition of P_d .

In energy space the dissipation process leads to a stationary flow of stars to highly negative values; at some point stars will be absorbed by the central black hole, for example by tidal disruption at the tidal radius r_t . As discussed in [Vilkoviskij & Czerny \(2002\)](#) the dissipation process will bring stars down into the plane of the disk, but two-body relaxation will reheat them in the vertical direction. Both effects drive the stars inwards to the black hole, where they are finally tidally disrupted and accreted. Here we use a simple parametrized model; stars are absorbed onto the central black hole at some accretion radius r_{acc} , for which we demand $R_d \gg r_{\text{acc}} \gg r_t$, but otherwise treat it as a free parameter, varied in our simulations later on.

For scaling purposes with particle number N in the simulations we use the standard half-mass relaxation time of [Spitzer \(1987\)](#):

$$t_{\text{rx}} = \frac{0.14N}{\ln(0.4N)} t_{\text{dyn}} \quad \text{with} \quad t_{\text{dyn}} = \sqrt{\frac{r_{\text{half}}^3}{GM_{\text{cl}}}}$$

where r_{half} is the half-mass radius of the CSC. The half-mass relaxation time t_{rx} is given in [Table 1](#) for a series of galactic nuclei covering the observed range of SMBH masses.

The local relaxation time t_{rc} due to two-body encounters is given by ([Binney & Tremaine 1987](#), Eq. (8-71))

$$\begin{aligned} t_{\text{rc}} &= \frac{0.34\sigma^3}{G^2 m_s \rho_s \ln \Lambda} \\ &= \frac{18 \text{Gyr}}{\ln \Lambda} \left(\frac{\sigma}{1 \text{km s}^{-1}} \right)^3 \left(\frac{1 M_\odot}{m_s} \right) \left(\frac{1 M_\odot \text{pc}^{-3}}{\rho_s} \right) \end{aligned} \quad (15)$$

with 1-D velocity dispersion σ , mean particle mass m_s , and density ρ_s of the CSC. This equation can be applied at each radius or to the central region of a system by using mean values inside some radius r and is also called the 'core relaxation time'. Inside the gravitational influence radius r_h of the black hole (which is in our model of the same order as the disk outer radius R_d) we assume $\sigma_\star^2 \propto r^{-1}$ and the standard Bahcall-Wolf density cusp solution for the stellar density profile in the CSC is $\rho \propto r^{-7/4}$ ([Bahcall & Wolf 1976](#)). Hence we get for the

local relaxation time (cf. Eq. 16) $t_{\text{rc}} \propto r^{1/4}$. For the galactic nuclei in Table 1 the core relaxation time at the influence radius $t_{\text{rc}}(r_{\text{h}})$ is a factor of 1.5 to 2 shorter than t_{rx} . This shows that 2-body relaxation in the central part of galactic nuclei is well represented by our confined model with a CSC mass only 10 times larger than the SMBH mass.

For comparison with measurements in our simulations, as described later, it is more practical to define a *global* dissipation time scale t_{diss} and a *global* dimensionless dissipative time scale η in the following way:

$$\begin{aligned} \eta &= t_{\text{diss}}/t_{\text{rx}} \\ t_{\text{diss}} &= \frac{E_k}{\dot{E}^{(sd)}} = \frac{M_{\text{cl}}\sigma_{\star}^2(r_{\text{acc}})}{2\dot{E}^{(sd)}} = \frac{GM_{\text{bh}}M_{\text{cl}}}{2r_{\text{acc}}\dot{E}^{(sd)}} \end{aligned} \quad (16)$$

Here E_k , with $2E_k = M_{\text{cl}}\sigma_{\star}^2(r_{\text{acc}}) = GM_{\text{cl}}M_{\text{bh}}/r_{\text{acc}}$, and $\dot{E}^{(sd)}$ are the total kinetic energy and total energy dissipation rate of all stars at the accretion radius. An accretion time scale for the black hole growth is defined by $t_{\text{acc}} = M_{\text{bh}}/\dot{M}_{\text{bh}}$, or in dimensionless form $\nu = t_{\text{acc}}/t_{\text{rx}}$. We remove stars at r_{acc} ; so in a stationary state the energy dissipation rate required at r_{acc} to sustain the black hole mass accretion rate is $\dot{E}^{(sd)} = \dot{M}_{\text{bh}}GM_{\text{bh}}/(2r_{\text{acc}})$. With equation 17 we get

$$\nu = \frac{t_{\text{acc}}}{t_{\text{rx}}} = \eta \frac{t_{\text{acc}}}{t_{\text{diss}}} = \eta \frac{M_{\text{bh}}}{\dot{M}_{\text{bh}}} \frac{\dot{E}^{(sd)}}{E_k} = \eta\mu_{\text{bh}} \quad (17)$$

Hence the black hole mass accretion rate does not depend on the choice of r_{acc} , as will be verified in our numerical simulations later.

3. The Numerical Model

For the high resolution direct N -body simulations of the CSC we used the specially developed ϕ GRAPE (= *Parallel Hermite Integration with GRAPE*) code. The program uses the 4-th order Hermite integration scheme for the particles with hierarchical individual block time-steps, together with the parallel usage of GRAPE6 (or nowadays the GPU - Graphics Processing Unit) cards for the hardware calculation of the acceleration \vec{a} and the first time derivative $\dot{\vec{a}}$ of the acceleration. The code itself and also the special GRAPE hardware is described in more detail in Harfst et al. (2007). For all the new calculations we use the dif-

ferent NVIDIA CUDA/GPU hardware which emulate the standard GRAPE library calls¹.

Here we mention briefly the most important features added to the Hermite scheme of the N -body ϕ GRAPE code in order to model the ram pressure dissipative force and the star accretion to the SMBH:

- A dissipative force routine, where we calculate the acceleration caused by the interaction with the gaseous disk \vec{a}_{d} (Eq. 20) and its first time derivative $\dot{\vec{a}}_{\text{d}}$.
- We reduce the time-steps of stars when they come close to the disk plane. Otherwise stars with big individual time step may miss the disk and would not feel the effect of the disk at all.
- A simple accretion scheme of stars onto the SMBH, where the stellar mass is added to the central black hole if they get inside a certain accretion radius. The accretion radius is used as a free scaling parameter; results for different accretion radii can be used to scale to real parameters of galactic nuclei (see 4.2). This algorithm has been described and used in Fiestas et al. (2011); Li et al. (2012).
- In order to control integration error we add a careful bookkeeping of energy changes caused by removing stars in process of accretion and by the dissipative force of the stars-gas interaction. In all our runs the total energy error does not exceed 10^{-4} .

In the simulations we use standard N -body units given by

$$G = M_{\text{cl}} = 4|E_{\text{tot}}| = 1, \quad (18)$$

where E_{tot} is the total energy of the initial Plummer sphere for the CSC without a perturbing SMBH (Heggie & Mathieu 1986). Note that in this scaling an increase of the particle number takes place at constant total mass; hence the stellar mass $m_{\star} \propto 1/N$ decreases with particle number, and it also decreases with respect to e.g. the disk mass and black hole mass.

¹<ftp://ftp.mao.kiev.ua/pub/users/berczik/STARDISK/>

Table 1: Some examples for the physical scaling of galactic nuclei.

Object	$M_{\text{bh}} [M_{\odot}]$	σ_c [km/s]	r_h [pc]	N	t_{dyn} [Myr]	t_{rx} [Gyr]	Q_{tot}	$Q_{\text{tot}}(8k)$	L_{max} [L_{\odot}]
M 87	6.6×10^9	312	291	6.6×10^{10}	1.5	6×10^5	2.1×10^{-9}	5.7×10^{-3}	1×10^8
NGC 3115	9.6×10^8	230	78	9.6×10^9	0.58	3.4×10^4	4.2×10^{-9}	1.8×10^{-3}	2.8×10^7
NGC 4291	3.2×10^8	242	24	3.2×10^9	0.16	3400	1.5×10^{-8}	2.4×10^{-3}	9.4×10^7
M 31	1.5×10^8	160	25	1.5×10^9	0.26	2690	6.2×10^{-9}	4.7×10^{-4}	5×10^7
NGC 4486A	1.3×10^7	111	4.5	1.3×10^8	0.067	68.8	1.7×10^{-8}	1.2×10^{-4}	1.9×10^8
MW	4×10^6	110	1.4	4×10^7	0.021	7.2	5.2×10^{-8}	1.2×10^{-4}	5×10^8
M 32	3×10^6	75	2.3	3×10^7	0.050	12.9	1.5×10^{-8}	2.8×10^{-5}	2×10^8

NOTE.—For the CSC we adopt $\mu_{\text{bh}} = 0.1$, solar-type stars with $m_{\star} = 1M_{\odot}$, $r_{\star} = 2.3 \times 10^{-8}$ pc, $v_{\text{esc}} = 620$ km/s, $R_d = r_h$ and $r_{\text{half}} = 3r_h$, and $Q_d = 5$ for the bow shock size. Most observational data (Cols. 2 and 3) are taken from Gültekin et al. (2009), improved values for M 87 are from Murphy et al. (2011), and M_{bh} for the Milky Way (MW) is from Gillessen et al. (2009). The influence radius (Col. 4) is derived from $r_h = GM_{\text{bh}}/\sigma_c^2$, with the core velocity dispersion σ_c of the CSC; N is the number of stars in the CSC derived from $M_{\text{bh}}/\mu_{\text{bh}}$, the dynamical and half-mass relaxation timescales (Cols. 6 and 7) are derived by Eq. 14, the physical and scaled cross sections Q_{tot} and $Q_{\text{tot}}(8k)$ (Cols. 8 and 9) by Eqs. 19 and 21, and the maximum luminosity by accretion (Col. 10) assuming $L_{\text{max}} = 0.1M_{\text{bh}}c^2$.

Our model consists of three components: the CSC, the SMBH, and the AD. The CSC with initial mass M_{cl} is realized by N particles of mass m_{\star} . The initial density distribution is a Plummer model, which is only in dynamical equilibrium if the gravity of the central SMBH is ignored. The system adjusts quickly in a few dynamical time scales. The mutual gravitational interactions and the dissipative force on the stars in the AD are calculated fully by the ϕ GRAPE code.

The SMBH with initial mass $M_{\text{bh}} = \mu_{\text{bh}}M_{\text{cl}}$ is modeled by an analytic Kepler potential fixed at the origin. We allow accretion of stars, which are effectively captured by the inner part of the AD or scattered by two-body relaxation into the loss cone, to grow the mass of the SMBH. Physically the accretion radius r_{acc} is given by the tidal radius r_t , where the stars are disrupted, or the Schwarzschild radius r_S . Both radii are orders of magnitude below our numerical resolution. Therefore we need to analyze the scaling of the accretion with decreasing accretion radius. The orbits of the stars accreted by the interaction with the AD are circularized before being accreted. In contrast, stars accreted by two-body scattering into the loss cone are predominantly accreted on hyperbolic orbits. In order to simulate the effect of the different eccentricity distribution, we apply a second accretion criterion based on the velocity of the stars. We define an accretion criterion to merge stars with the SMBH using two criteria: 1) distance $r < r_{\text{acc}}$ and 2) $V_{\star}^2 < k_{\text{acc}}v_{\text{circ}}^2$. Stars well inside the influence radius of the SMBH are

moving on (local) Kepler orbits, where the velocity is given by $V_{\star}^2 = v_{\text{circ}}^2(2 - r/a)$ with semi-major axis a . In the limit of large k_{acc} all stars reaching r_{acc} would be accreted. For $k_{\text{acc}} = 1$ stars inside r_{acc} are accreted, if $a \leq r_{\text{acc}}$, i.e. all stars with energy below $-GM_{\text{cl}}/r_{\text{acc}}$ (neglecting the potential energy of the CSC) are accreted in one orbital time. In all simulations we use $k_{\text{acc}} = 1$. (Note for completeness that in some runs with AD we accreted all stars with $r < r_{\text{acc}}/10$ independent of their energy. We have tested that the accretion rates are not changed significantly by this additional accretion criterion.)

The properties of the AD are fixed by the normalized mass μ_d with analytic density distribution according to Eq. 6 with $\alpha = 3/4$, $s = 4$, and constant thickness $h = 10^{-3}$. We use a Kepler rotation of the AD in the potential of the SMBH neglecting the gravity of the CSC and pressure gradients in the AD. We set the outer cutoff initially at $R_d = r_h$. Using a Kepler rotation curve underestimates the real circular speed at the outer boundary by a factor of 1.4, but this has no significant influence on the dynamics of the stars. The reason is that the gas density and thus the friction force is very small in the outer regions of the AD. The part of the AD with significant dissipation of energy of crossing stars is deep inside the influence radius of the SMBH. Here the approximation of Kepler rotation is very good. We have chosen the large cutoff radius only in order to avoid another free parameter.

It is helpful for calibration of our models with

respect to real systems in galactic nuclei to define an effective dissipative parameter

$$Q_{\text{tot}} = Q_{\text{d}} \frac{N\pi r_{\star}^2}{\pi R_{\text{d}}^2}. \quad (19)$$

Note that Q_{tot} enhances Q_{d} by a factor, which describes the dimensionless total dissipative cross section of N stars, normalized to the disk area. With this definition we can rewrite the original dissipative force in Eq. 10 as acceleration

$$\vec{a}_{\text{d}} = \vec{F}_{\text{d}}/m_{\star} = -Q_{\text{tot}} \frac{\pi R_{\text{d}}^2 \rho_{\text{g}}}{M_{\text{cl}}} |\vec{V}_{\text{rel}}| \vec{V}_{\text{rel}}. \quad (20)$$

The *local* parameters like r_{\star} , m_{\star} , and Q_{d} , whose scaling in terms of N -body units is not straightforward, are transformed in this way to the *global* quantities such as R_{d} , M_{cl} , and Q_{tot} .

Due to numerical limitations, direct N -body simulations are performed here with particle numbers smaller than that in a real galactic nucleus. This leads to the relaxation time being a function of the particle number, N , whereas it is a fixed quantity for a given nucleus. To correct for this, the simulations are run for a multiple of the relaxation time and are then rescaled to the correct time units to compare to a physical galactic nucleus. For this reason, all physical processes, including the star-disc drag, need to be rescaled as well. In our models all quantities except Q_{tot} are invariant when changing the particle number in the simulation. Therefore for calibration to real systems we just have to compute the value of Q_{tot} and adjust it correspondingly in our model system. But this step alone is not sufficient; our model system has a much shorter two-body relaxation time than in reality. We want to study numerical systems at smaller particle number, which have all the same ratio η of dissipation to relaxation time scale. Therefore we need to choose Q_{tot} such that the same value for η is achieved:

$$Q_{\text{tot}}(N_2) = \frac{t_{\text{rx}}(N_1)}{t_{\text{rx}}(N_2)} Q_{\text{tot}}(N_1) \quad (21)$$

Our model aims to discover numerically the secular evolution of the coupled star gas system in galactic nuclei. Therefore we are interested in the interplay between dissipative processes (star-gas drag) and two-body relaxation processes - the semi-analytic model of Vilkoviskij & Czerny

(2002) defines the setup in which we want to put our numerical models. Since we are not yet able to simulate star-by-star, two different effects have to be taken into account for this: (i) each simulation particle effectively represents many stars, not a single star. Therefore we cannot study the individual star-gas drag effects here, only the collective one; this is shown by the definition of Q_{tot} in Eq. 19, which shows how for one simulation particle an effective cross section is realized, which corresponds to the effect of the much larger stellar system we have in mind. (ii) In our system with lower particle number the two-body relaxation time has a “wrong” ratio to other time scales. Therefore, we rescale Q_{tot} in such a way, that the relaxation time and the dissipation time have the correct ratio for the larger system, which is done in the Eq. 21. Eq. 21 shows, for example, that for a system with 10^8 particles, to be simulated by only $N = 10^4$, we need to increase Q_{tot} artificially by a factor of $\sim 5,000$. In Table 1 the real values of Q_{tot} and simulated values for $N = 8000$ are both given for the selected galaxies. It should be stressed that we do NOT intend to model star-gas interactions in detail. Rather we apply a standard model of it, scale it up in a collective way and calibrate it with respect to the relaxation time. Our main goal is to check the increase of star accretion rates due to the presence of a central AD.

In our starting configuration we added the central SMBH to the Plummer distribution of the CSC. In order to start the analysis of the system in dynamical equilibrium we let the CSC evolve for $\sim 5t_{\text{dyn}}$ with the SMBH. After the initializing phase the cusp around the SMBH shows a density slope $\gamma \approx 2.5$ which still differs from a BW cusp (top panel of Fig. 2). The difference of the set-up Plummer profile and the cumulative mass profile at $t = 0$ demonstrates the effect of virialization in the potential of the SMBH. Then we determine R_{d} such that at $t = 0$ the enclosed CSC mass at $R = R_{\text{d}}$ equals the SMBH mass.

We performed a series of simulations combining different particle numbers $N = 4k, 8k, 16k$ and different accretion radii $r_{\text{acc}} = 0.04, 0.02, 0.01, 0.005$ (see Table 2) until $t = 10t_{\text{rx}}$. The identifiers of the simulations in Table 2 are coding the particle number and accretion radius. For each parameter combination a run without dissipative force is done for comparison. For the different N we

Table 2: Model parameters of all runs.

Model	N	ϵ/R_d	r_{acc}/R_d	$Q_{\text{tot}}(N)$
04K-005	4k	4.55×10^{-4}	5×10^{-3}	10^{-2}
04K-01	4k	4.55×10^{-4}	10^{-2}	10^{-2}
04K-02	4k	4.55×10^{-4}	2×10^{-2}	10^{-2}
04K-04	4k	4.55×10^{-4}	4×10^{-2}	10^{-2}
08K-005	8k	4.55×10^{-4}	5×10^{-3}	5.47×10^{-3}
08K-01	8k	4.55×10^{-4}	10^{-2}	5.47×10^{-3}
08K-02	8k	4.55×10^{-4}	2×10^{-2}	5.47×10^{-3}
08K-04	8k	4.55×10^{-4}	4×10^{-2}	5.47×10^{-3}
16K-005	16k	4.55×10^{-4}	5×10^{-3}	2.97×10^{-3}
16K-01	16k	4.55×10^{-4}	10^{-2}	2.97×10^{-3}
16K-02	16k	4.55×10^{-4}	2×10^{-2}	2.97×10^{-3}
16K-04	16k	4.55×10^{-4}	4×10^{-2}	2.97×10^{-3}

NOTE.—Column 1 gives the identification label of the model, columns 2–4 are number of particles, smoothing length and accretion radius. Column 5 gives the total cross section, Q_{tot} , scaled according to Eq. 21. Common parameters for all models are $\mu_{\text{bh}} = 0.1$, $\mu_d = 0.01$, $h = 10^{-3}$, $k_{\text{acc}} = 1$.

applied the scaling according to equation 21. For the simulations with dissipative force our choice of Q_{tot} corresponds to the case of M 87 (compare Tables 1 and 2). From the last column in Table 1 it is obvious that for lower mass black holes the value of Q_{tot} in our simulations is unrealistically large.

For the calculation of the CSC dynamics we used the parallel GRAPE systems built at the Astronomisches Rechen-Institut in Heidelberg², and at the Fesenkov Astrophysical Institute in Almaty. The code has recently been ported to large clusters with GPU hardware (in Beijing, China and Heidelberg, Germany, see acknowledgments) and results from these facilities have partly been used for this project.

4. Results

In our starting configuration the CSC is in dynamical equilibrium including the gravitational potential of the SMBH and has a steep cusp in the density profile. The cumulative mass profiles in the top panel of Fig. 2) shows that after one relaxation time the BW cusp is in place and remains stable over the full simulation. The lower panel of Fig. 2 shows the Lagrange radii of the CSC for 1, 5, 25, 50, 90, 99 percent enclosed mass with respect

to the total mass $M_{\text{cl}}(t)$ for the model 16K-005 (see Table 2 for model parameters). Additionally the position of the innermost particle (1p) shows that stars crossing r_{acc} on highly eccentric orbits are quickly circularized and accreted. The influence radius r_h of the SMBH is increasing during the simulation by an order of magnitude due to accretion and the size of the Bahcall-Wolf cusp is growing accordingly.

4.1. Scaling with particle number

In simulations without AD, stars reaching r_{acc} are immediately accreted onto the SMBH. The corresponding loss-cone in phase space has a maximum angular momentum for each energy defining the opening angle of the loss cone in phase space. The regime of an empty loss cone depends on $t_{\text{rx}}/t_{\text{dyn}}$ and the width of the loss cone (Amaro-Seoane & Spurzem 2001). In the regime with a high probability of a star to be scattered in or out of the loss-cone, the loss cone is full. In the empty loss-cone regime all stars scattered by two-body encounters into the loss cone are accreted and the accretion rate scales with t_{rx} . In the full loss cone regime the accretion rate depends on t_{dyn} . In a given system the empty part of the loss cone increases with increasing particle number N leading to a N dependence of the accretion rate. We used an additional energy criterion accreting

²GRACE: <http://www.ari.uni-heidelberg.de/grace>

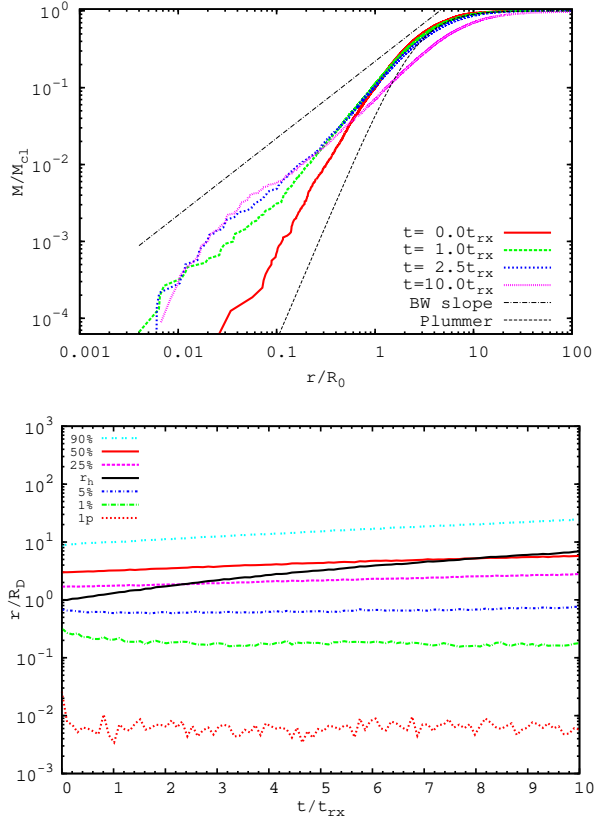


Fig. 2.— Evolution of the CSC for model 16K-005. Top panel: Cumulative mass profiles in units of the initial CSC mass at different times with the Plummer profile and the power law of a Bahcall-Wolf (BW) cusp added for comparison. Bottom panel: Lagrange radii enclosing a fixed mass fraction with respect to $M_{e1}(t)$. The position of the inner-most particle (1p) and the influence radius r_h are also shown.

stars with semi-major axis $a < r_{acc}$, which cuts the loss-cone in energy space.

In Fig. 3 the lower set of thin lines show the growing mass of the SMBH for different particle numbers for the cases without dissipation due to the AD (top panel: $r_{acc} = 0.04$ and bottom panel: $r_{acc} = 0.005$). The accretion rate per relaxation time is seen to slowly increase with particle number. The upper set of thick lines in Fig. 3 show that accretion is significantly larger when the dissipative force of the AD is included. The accretion rate is found to be independent of particle number N . In Fig. 4 the ratio of the accretion rates with and without dissipative force is quantified for the $8k$ simulations at different accretion radii. After a few relaxation times an equilibrium with an enhancement factor of ~ 4 is established for all accretion radii.

4.2. The accretion radius

The physical accretion radius r_{acc} is much smaller than the numerical resolution. Therefore the scaling of the accretion rate with r_{acc} is very important. Without the AD the standard loss cone becomes thinner with decreasing r_{acc} , leading to a decreasing accretion rate in the limit of an empty loss cone (e.g. Amaro-Seoane & Spurzem 2001). On the other hand the Bahcall-Wolf cusp is characterized by a constant mass and energy flow to the SMBH and high binding energy, respectively. As a consequence the accretion rate based on an energy criterion should be independent of r_{acc} . In Fig. 5 the independence of the accretion rate in terms of the accretion timescale ν (Eq. 17) on r_{acc} is shown for all $N = 16k$ runs with dissipative force. For $t > 1 t_{tx}$ the accretion rate is also independent of the particle number N .

With the chosen parameters for the AD and the CSC the growth timescale of the SMBH by accretion of stars is of the order of the half-mass relaxation time t_{rx} of the CSC, which is long compared to the Eddington accretion timescale of ≈ 50 Myr (see Table 1). Therefore our model applies to quiescent galactic nuclei. The accretion rate can be converted to a maximum luminosity by adopting $L_{max} = 0.1 \dot{M}_{bh} c^2$. This upper limit is for all SMBH masses in the range of $2 \dots 50 \times 10^7 L_{\odot}$ (last column of Table 1).

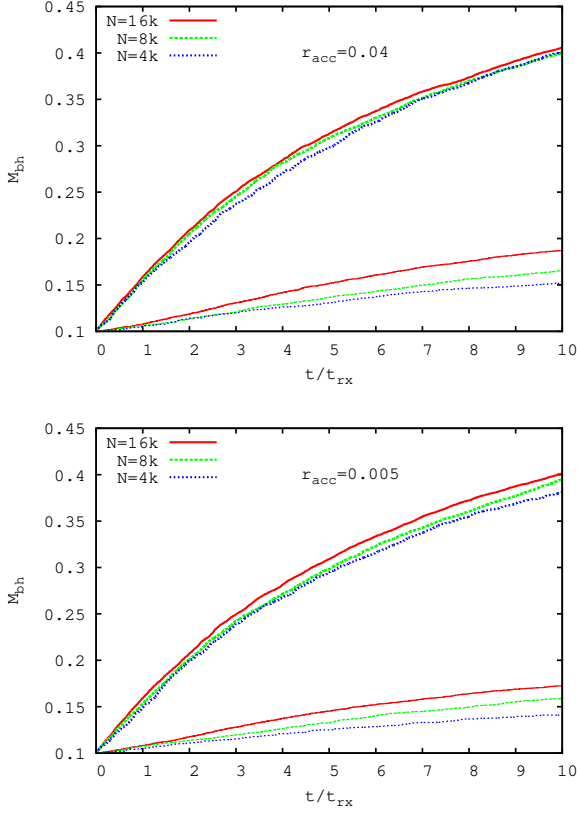


Fig. 3.— SMBH growth with (upper thick lines) and without (lower thin lines) dissipative force for different accretion radii $r_{\text{acc}} = 0.04$ (top panel) and $r_{\text{acc}} = 0.005$ (bottom panel). The particle number ranges from $N=4k\dots 16k$. Q_{tot} scales according to Eq. 21 with N .

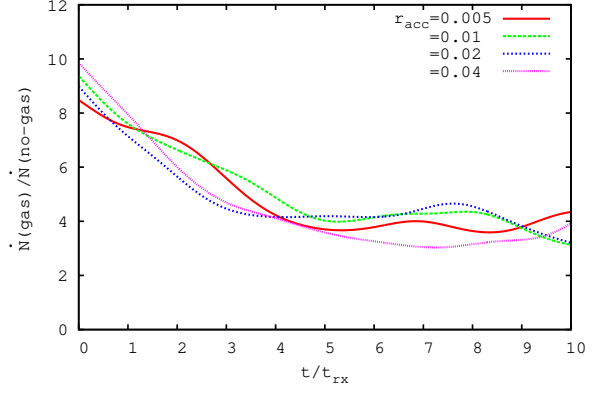


Fig. 4.— Ratio of the accretion rates with and without dissipative force for $N=8k$ and different r_{acc} .

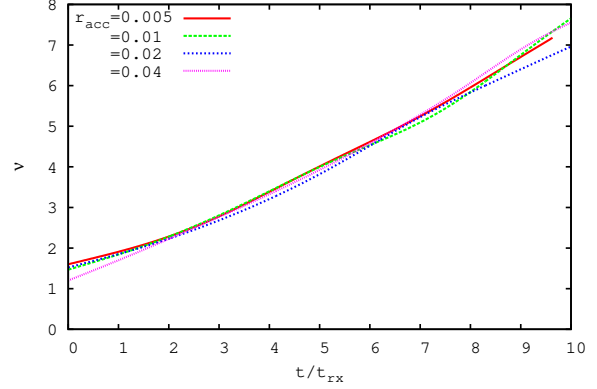


Fig. 5.— Normalized accretion timescale ν (Eq. 17) for $N = 16k$ with different r_{acc} (same line-styles as in Fig. 4).

4.3. Energy dissipation

Our measurement of the *global* normalized dissipative time scale η in the simulations uses the definition as given in Eq. 17.

In a stationary state the time scale of transport of stars through the AD towards the black hole is dominated by the outer edge of the disk, where the dissipation time scale is longest. Therefore, a measurement of the total dissipated energy in our system should not depend on the choice of r_{acc} , where we actually remove the stars and add their mass to the central SMBH, as it has been shown by Eq. 17. The normalized dissipation timescale η is a measure of the dissipated energy. It is determined by the numerical evaluation of $E_{\text{kin}}(t)$ and $\dot{E}^{(\text{sd})}(t)$, the latter via smoothing of the cumulative function $E^{(\text{sd})}(t)$ to derive the slope. After an initial adaption phase η is approximately constant (Fig. 6) showing the constant energy flow in a stationary BW cusp. As seen in Fig. 6, the normalized dissipation timescale is independent of N and depends only weakly on r_{acc} . The long-term trend of increasing η is due to the evolution of the SMBH and the CSC by the accretion of stars. The SMBH mass is increasing and the mass of the CSC is decreasing leading to an increasing μ_{bh} and virial factor ξ_{k} , and a decreasing total cross section Q_{tot} and efficiency P_{d} with time. By comparing the dissipation timescale η shown in Fig. 6 and the accretion timescale ν shown in Fig. 5 we observe that the relation derived in Eq. 17 is approximately fulfilled (taking into account the growth of the black hole and the decreasing CSC mass for μ_{bh}).

5. Discussion and Conclusions

In galactic nuclei super-massive black holes co-exist with a dense stellar cluster; galaxy mergers and the quasar phenomenon indicate that at least for some time there should be also large amounts of interstellar gas present in the nuclear regions around the black holes. In this paper we have examined the interaction and co-evolution of a dense star cluster surrounding a star-accreting super-massive black hole with an assumed central gaseous disk. Interactions of such disks with the surrounding dense star clusters have been proposed as source of gas supply to the central disk (Miralda-Escudé & Kollmeier 2005), as

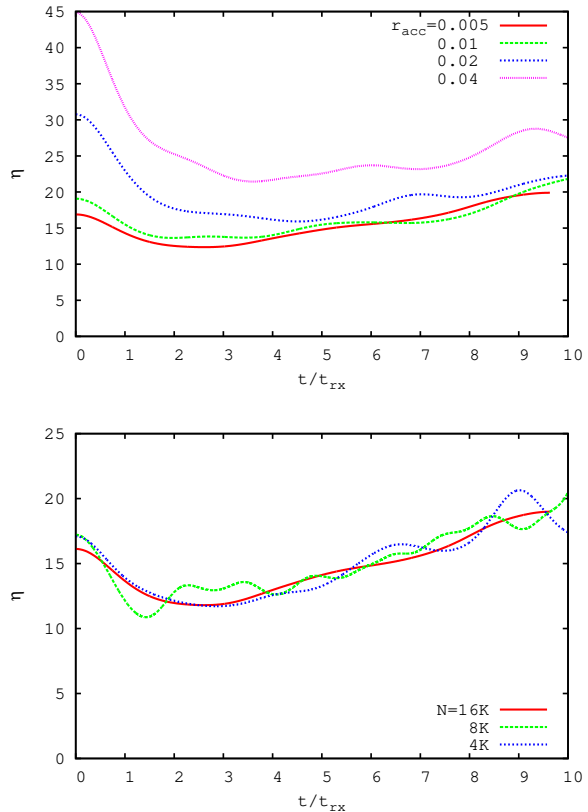


Fig. 6.— Normalized dissipation timescale η (Eq. 17) for $N = 16k$ and different r_{acc} (top panel) and for $r_{\text{acc}} = 0.005$ and different N (bottom panel).

agents to enhance the tidal star accretion rate (Vilkoviskij & Czerny 2002), and to cause feedback on the orbital parameters of stars (Rauch 1995), including a modification of sources of gravitational waves (Rauch 1999).

Our model is the first self-consistent long-term simulation of a dense star cluster, surrounding a star-accreting super-massive black hole, and subjecting the stars to the dissipative forces from a resolved central gaseous disk. We resolve effects of two-body relaxation, dissipation of stellar kinetic energy in the disk and star accretion onto the central black hole in a numerical study based on direct high-accuracy simulations. Since star-by-star modeling of a galactic nucleus down to the realistic tidal radius is not yet possible, despite of the modern GPU hardware used for simulations, a careful scaling analysis is presented as a function of the particle number in the simulations and of an assumed star accretion radius, to allow conclusions for the real astrophysical situation in galactic nuclei. But our model still has a number of serious drawbacks. Firstly, it assumes a stationary accretion disk, so energetic feedback to the disk structure by star-disk interactions is neglected, secondly, the physics of star-gas interactions is modeled approximately. Finally, there is no distinction between properties of different stars (main sequence, giants, remnants), but rather a single stellar species with solar radius is assumed. In that sense our study should be considered as a pathfinder and exploratory.

This investigation is a direct continuation of a semi-analytic study by Vilkoviskij & Czerny (2002), extending it by a more detailed and numerical study of the stellar dynamical evolution of the central stellar cluster. Our paper uses a numerical approach based on direct N -body simulations, including particle-particle forces as well as a dissipative force in the disk. Here we resolve the dissipation of stellar kinetic energy along the stellar paths in the vertically extended accretion disk. Particle numbers in our simulations and an adopted star accretion radius (onto the central super-massive black hole) are used as free parameters in our model, while for other important parameters of the problem fiducial values are assumed. These are e.g. the initial super-massive black hole mass (10 percent of the initial central stellar cluster mass), the gaseous accretion disk

mass (10 percent of the initial black hole mass), and the outer radius of the accretion disk (set equal to the black hole gravitational influence radius). Finally, all star particles are equal in the simulation, and their total effective cross section is used as a parameter to obtain the physically correct ratio of dissipation to relaxation time.

We show that the accretion rate of stars onto the super-massive black hole is strongly enhanced by the dissipative force of the accretion disk (a factor of four with our parameters). The accretion process is determined by an equilibrium of diffusion by two-body encounters and energy loss by the dissipative force. Consistently there is also an energy deposition in the central accretion disk; we find that most stars accreted or trapped in the disk are quickly accreted also to the black hole, because there is no stable co-rotation of the stars with the disk. Our results are robust with respect to variation of particle number and adopted accretion radius, therefore they should hold under realistic conditions in galactic nuclei. Our star accretion rate does not depend strongly on the adopted star accretion radius; it supports the idea of Vilkoviskij & Czerny (2002), that there is a stationary flow of stars within the disk towards the central black hole, which is determined by an equilibrium between dissipation and relaxation time. In spite of the enhanced number of stars accreted through the disk, we still find that there is a Bahcall-Wolf central density cusp present in the system, which is not significantly perturbed.

Central densities in star clusters near super-massive black holes can reach $10^8 M_{\odot} \text{pc}^{-3}$ or more. At such high stellar densities direct, disruptive stellar collisions may produce gas in the gravitational potential well of the black hole. The gas production rate could be larger than the one obtained from tidal disruption of stars (Spitzer & Saslaw 1966; Spitzer & Stone 1967); see also Begelman & Rees (1978); Frank & Rees (1976), and numerical models in e.g. Freitag & Benz (2002); Freitag, Gürkan & Rasio (2006); Freitag, Rasio & Baumgardt (2006). But there is little doubt that a large fraction of this gas is finally accreted to the SMBH; some fraction of it though may escape. The same is true for the gas produced by tidal accretion. Our models do not yet resolve the very central regions of the star cluster, where stellar collisions may occur predominantly. We anyway treat the ac-

cretion radius as a free parameter used for scaling studies; it is here usually large compared to the astrophysically defined tidal radius, where stars are destroyed by tidal forces. Our results should not depend strongly on whether the stars inside r_{acc} are finally disrupted by tidal forces or destroyed by stellar collisions with subsequent accretion of the gas onto the SMBH. Less is known about the effect of induced stellar collisions due to low relative velocities of stars in the disk (due to dissipation). We will study the effects of direct stellar collisions in future work.

Direct stellar collisions produce another source of gas deep in the gravitational well of the central supermassive black hole. As in the case of tidal disruptions of stars, we do not know exactly how much mass is accreted to the SMBH, and how much is ejected due to magnetic fields (jets) and radiation pressure near it (see e.g. one improved model by Kasen & Ramirez-Ruiz 2010). Our assumption to add 100% of the material from tidal accretion to the black hole clearly is an upper limit, the real growth rate may be lower due to some mass loss in the process, also for stellar collisions. However, even in our case with possibly overestimated accretion rates, assuming a typical value of 10% mass to energy conversion, the luminosity obtained from our mass accretion rates are of the order of $10^8 L_{\odot}$, much smaller than the Eddington luminosity. Therefore our results are applicable to quiescent galactic nuclei, not to quasars or AGN in their most active phase, where high mass accretion rates, feedback and outflows are driven for example by gas inflow due to galaxy mergers.

The response of the central accretion disk to the deposition of energy and stars is neglected in this paper. We will work on this problem in future studies. The black hole growth rate due to star accretion will be limited by the condition that the accretion disk can find a new equilibrium absorbing the dissipated stellar energy and radiating it. In the inner spherically symmetric part of the system the Eddington limit will pose an upper limit to the star accretion rate allowed in a stationary state (see discussion by Miralda-Escudé & Kollmeier 2005). In that sense our accretion rates, determined by neglecting feedback on the disk, will be upper limits. It is still possible that the process of star trapping to the

disk and star and gas accretion to the central black hole is quasi-periodic and highly non-stationary (as suggested by the ubiquitous time variability of radiation from active galactic nuclei).

Acknowledgments

This work has been made possible by Volkswagen Foundation under the project “STARDISK – Simulating Dense Star-Gas Systems in Galactic Nuclei using special hardware” (I/81 396), for supporting collaboration with science and education in Kazakhstan. We acknowledge personal support for DY and MM and support for German-Kazakhstan exchange and cooperation for our entire author team. Finally, GRAPE and GPU hardware at Fesenkov Astrophysical Institute in Kazakhstan used for this work has been supported by the STARDISK project.

Simulations were also performed on the GRACE supercomputer (grants I/80 041-043 and I/81 396 of the Volkswagen Foundation and 823.219-439/30 and /36 of the Ministry of Science, Research and the Arts of Baden-Württemberg) and the special supercomputer Laohu at the High Performance Computing Center at National Astronomical Observatories, funded by the Ministry of Finance of China under the grant ZDYZ2008-2, has been used. RS and PB acknowledge support by the Chinese Academy of Sciences through Grant Number 2009S1-5 (The Silk Road Project).

PB acknowledges the special support by the NASU under the Main Astronomical Observatory GRID/GPU computing cluster project. PB’s studies are also partially supported by the program Cosmomicrophysics of NASU. A careful reading of the preprint by Luca Naso was very helpful. We thank the anonymous referee for an intensive discussion which led to major clarifications of the methods and approximations used.

REFERENCES

- Aarseth S.J., 1999a, *PASP*, 111, 1333
- Aarseth S.J., 1999b, *Cel. Mech. Dyn. Astron.*, 73, 127
- Amaro-Seoane, P., Spurzem, R. 2001, *MNRAS*, 327, 995

- Amaro-Seoane, P., Freitag, M., Spurzem, R. 2004, MNRAS, 352, 655
- Artymowicz P., Lin, D.C.N., Wampler E.J., 1993, ApJ, 409, 592
- Bahcall J.N., Wolf R.A., 1976, ApJ, 206, 214
- Begelman M. C., Rees M. J., 1978, MNRAS, 185, 847
- Binney J., Tremaine S., 1987, Galactic Dynamics, Princeton Univ. Press, New Jersey, USA
- Baruteau, C., Cuadra, J., Lin, D. N. C., 2011, ApJ, 726, 28
- Bisnovatyi-Kogan G.S. & Syunyaev R.A., 1972, SovA, 16, 201
- Bisnovatyi-Kogan G.S., 1978, Astronomy Lett., 4, 130
- Callegari, S., Kazantzidis, S., Mayer, L., Colpi, M., Bellovary, J. M., Quinn, T., Wadsley, J., 2011, ApJ, 729, 85
- Callegari, S., Mayer, L., Kazantzidis, S., Colpi, M., Governato, F., Quinn, T., Wadsley, J., 2009, ApJ, 696, L89
- Colgate S.A., 1967, ApJ, 150, 163
- Cuadra, J., Armitage, P. J., Alexander, R. D., Begelman, M. C. MNRAS, 393, 1423
- Fiestas J., Porth O., Berczik P., Spurzem R., 2011, MNRAS, 419, 57
- Frank J., Rees M., 1976, MNRAS, 176, 633
- Frank J., King A., Raine D., 2002, 3rd Ed. Cambridge University Press, 2002
- Freitag, M., Benz, W., 2002, A&A, 394, 345
- Freitag M., Gürkan M. A., Rasio F. A., 2006, MNRAS, 368, 141
- Freitag M., Rasio F. A., Baumgardt H., 2006, MNRAS, 368, 121
- Gillessen, S., Eisenhauer, F., Trippe, S., Alexander, T., Genzel, R., Martins, F., Ott, T., 2009, ApJ, 692, 1075
- Gültekin, K., et al., 2009, ApJ, 698, 198
- Gurevich, A.V., 1964, Geomagnetism and Aeronomy 4, 192
- Hara T., 1978, Prog. Theor. Phys., 60, 711
- Harfst S., Gualandris A., Merritt D., Spurzem R., Portegies Zwart S., Berczik P., 2007, New A, 12, 357
- Heggie, D.C. and Mathieu, R.D., 1986. In *The Use of Supercomputers in Stellar Dynamics*, p. 233, ed. Hut, P. and McMillan, S., Springer-Verlag, New York.
- Hills J. G., 1975, AJ, 80, 1075
- Just, A., Khan, F.M., Berczik, P., Ernst, A., Spurzem, R., 2011, MNRAS, 411, 653
- Kasen D., Ramirez-Ruiz E., 2010, ApJ, 714, 155
- Kormendy J., Richstone D., 1995, ARA&A, 33, 581
- Langbein T., Spurzem R., Fricke K.J., Yorke, H.W., 1990, A&A, 227, 333
- Li S., Liu F.K., Berczik P., Chen X., Spurzem R., 2012, ApJ, 748, 65
- Lightman, A.P., Shapiro, S.L., 1976, Nature, 262, 743
- Miralda-Escudé J., Kollmeier J.A., 2005, ApJ, 619, 30
- Murphy, J., Gebhardt, K., Adams, J. 2011, ApJ, 729, 129
- Novikov, I., Thorne, K.S., 1973, in Black Holes, ed. C. de Witt & B.S. de Witt (Gordon & Breach, NY), 436
- Ostriker, E.C., 1999, ApJ, 513, 252
- Park, M.G., Ostriker, J.P., 2001, ApJ, 549, 100
- Rauch K.P., 1995, MNRAS, 275, 628
- Rauch K.P., 1999, ApJ, 514, 725
- Rees, M.J. 1984, ARA&A22, 471
- Sanders, R.H. 1970, ApJ162, 791
- Shakura, N.I., Sunyaev, R.A., 1973, A&A, 24, 337

- Spitzer, L., 1987, Dynamical Evolution of Globular Clusters, Princeton
- Spitzer, L.Jr., 1969, ApJ, 158, L139.
- Spitzer L.Jr., Saslaw W. C., 1966, ApJ, 143, 400
- Spitzer, L.Jr., Stone, M.E. 1967, ApJ147, 519
- Spurzem R., 1999, J. Comp. Appl. Math., 109, 407
- Spurzem R., Berczik, P., Hensler, G., Theis, Ch., Amaro-Seoane, P., Freitag, M., Just, A., 2004, PASA, 21, 188
- Spurzem R., Deiters S., Fiestas J., 2003, in “New Horizons in Globular Cluster Astronomy”, G. Piotto, G. Meylan, G. Djorgovski, M. Riello (eds.), ASP Conf. Ser., 296, 45
- Šubr L., Karas V., Huré J.-M., 2004, MNRAS, 354, 1177
- Šubr L., Karas V., 1999, A&A, 352, 452
- Sugimoto D., Chikada Y., Makino J., Ito T., Ebisuzaki T., Umemura M., 1990, Nature, 345, 33
- Syer D., Clarke C.J, and Rees M.J., 1991, MNRAS, 250, 505
- Vilkoviskij E.Y., 1975, Astrophys. Lett., 1, 8
- Vilkoviskij E.Y., and Bekbosarov N., in: KazGU Proc., Alma-Ata, 1982, 100
- Vilkoviskij E.Y., 1983, Astrophys. Lett., 9, 405
- Vilkoviskij E.Y., Czerny B., 2002, A&A387, 804
- Vokrouhlicky D., Karas V., 1998, MNRAS, 298, 53.